

*Dedicated*

*To*

*My Beloved Family*

## CERTIFICATE

It is certified that the work contained in the thesis titled "STUDY OF SrTiO<sub>3</sub> BASED ANODE MATERIALS FOR INTERMEDIATE TEMPERATURE SOLID OXIDE FUEL CELL" by "SAURABH SINGH" has been carried out under my supervision and that this work has not been submitted elsewhere for a degree.

It is further certified that the student has fulfilled all the requirements of Comprehensive Examination, Candidacy and SOTA for the award of Ph.D. Degree.



4/7/19

Supervisor

(Prof. Prabhakar Singh)


Dr. Prabhakar Singh  
प्रबोध/Professor  
भौतिकी विभाग/Dept. of Physics  
आर.पी.एस. (आर.पी.एस.)/IT (BHU)  
वाराणसी Varanasi-221005

## DECLARATION BY THE CANDIDATE

I, "SAURABH SINGH", certify that the work embodied in this thesis is my own bonafide work and carried out by me under the supervision of "PROF. PRABHAKAR SINGH" from JULY, 2013 to JULY, 2018 at the "DEPARTMENT OF PHYSICS", Indian Institute of Technology (BHU), Varanasi. The matter embodied in this thesis has not been submitted for the award of any other degree/diploma. I declare that I have faithfully acknowledged and given credits to the research workers wherever their works have been cited in my work in this thesis. I further declare that I have not willfully copied any other's work, paragraphs, text, data, results, etc., reported in journals, books, magazines, reports, dissertations, theses, etc., or available at websites and have not included them in this thesis and have not cited as my own work.


Date: 04/07/2018


Place: Varanasi

  
Signature of the Student  
(SAURABH SINGH)

## CERTIFICATE BY THE SUPERVISOR

It is certified that the above statement made by the student is correct to the best of my/our knowledge.

  
Supervisor  
(Prof. Prabhakar Singh)  
Dr. Prabhakar Singh  
प्राचार्य / Professor  
भौतिकी विभाग / Dept. of Physics  
भा.पौ.सं. (कां.हि.वि.) / IIT (BHU)  
वाराणसी / Varanasi-221005

  
Signature of Head of Department  
HEAD / विभागाध्यक्ष  
भौतिकी विभाग / Dept. of Physics  
भा.पौ.सं. (कां.हि.वि.) / IIT (BHU)  
वाराणसी / Varanasi-221005

## COPYRIGHT TRANSFER CERTIFICATE

**Title of the Thesis: Study of SrTiO<sub>3</sub> Based Anode Materials for Intermediate Temperature Solid Oxide Fuel Cell**

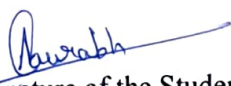
**Name of the Student: Saurabh Singh**

### Copyright Transfer

**The undersigned hereby assigns to the Indian Institute of Technology (Banaras Hindu University), Varanasi all rights under copyright that may exist in and for the above thesis submitted for the award of the “DOCTOR OF PHILOSOPHY”.**

Date: 04/07/2018

Place: Varanasi

  
Signature of the Student  
(SAURABH SINGH)

**Note: However, the author may reproduce or authorize others to reproduce material extracted verbatim from the thesis or derivative of the thesis for author's personal use provided that the source and the Institute's copyright notice are indicated.**

## ACKNOWLEDGEMENTS

---

It gives me immense pleasure to get an opportunity to express my heartfelt gratitude towards my respected supervisor, **Prof. Prabhakar Singh**, for his enthusiastic encouragement, guidance, support and valuable suggestions throughout my research work. His constant monitoring and interest in my work over the last five years will always remain as a happy memory. I will always remain thankful to him.

I express my gratitude to Prof. Bholanath Dwivedi, Prof. Onkar Nath Singh, Prof. Debaprasad Giri and Prof. Prabhakar Singh (Head of the Department) for their wholehearted support.

I also wish to thank my RPEC members Prof. Sandip Chatterjee, Assoc. Prof. Akhilesh Kumar Singh for the invaluable inspiration and numerous insightful suggestions during the entire course of this research.

I am thankful to Prof. A. S. K. Sinha, Department of Chemical Engineering and Technology for providing me required XPS facility and Prof. Incharge of CIFC, IIT(BHU) Varanasi for extending experimental facilities during the entire course of this research work.

I am very grateful to the Scientists Dr. Massimo Viviani (CNR-ICMATE, Genova, Italy), Dr. Sabrina Presto (CNR-ICMATE, Genova, Italy) and Dr. Salil Varma (BARC, Mumbai) for providing Instrumental Facilities as per characterizations of the samples. I would like to express my great appreciation for their valuable and constructive suggestions during the research work.

I would like to express my gratitude towards faculty members Prof. B.N. Dwivedi, Prof. O.N. Singh, Prof. D. Giri, Prof. S. Chatterjee, Prof. R. Prasad, Dr. A. Mohan, Dr. P. C. Pandey, Dr. S. Upadhyay, Dr. S. K. Mishra, Dr. S. Patil, Dr. Neha Agnihotri and Dr. S. Mishra for their valuable suggestions and help time to time in my research period.

I am also appreciative to Dr. Sunil Singh, Dr. Avanish Singh Parmar, Dr. Rajeev Singh, Dr. A. K. Srivastava, Dr. Saurabh Tripathi and Dr. P. Dutta for their kind encouragements and motivation. I am also thankful to all the technical, non-teaching as well as official staffs of the Department of Physics, IIT(BHU) Varanasi for their assistance when needed and also for providing me humorous relief at times.

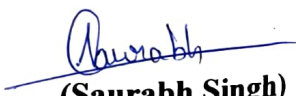
I would also like to express my extreme gratefulness towards my senior research members Dr. N. K. Singh, Dr. R. K. Singh, Dr. A. K. Yadav, Dr. Raghvendra, Dr. B. P. Singh, Dr. Pravin Kumar, Dr. Onkar nath Verma and all research colleagues of the lab for sharing their knowledge and creating enjoyable lab atmosphere both on and off the slopes. Special thanks are due to all the my departmental research colleagues and seniors Dr. Gaurav Gautam, Mr. Abhishek Singh, Dr. Pradeep Kumar, Mr. Rahul Singh, Mr. Prince Gupta, Mr. V. N. Mishra, and Mr. Pawan Kumar for the help and their awesome company for giving me moral support, pleasant company and confidence to complete my work with a 'smile'.

The cooperation, moral support and constant motivation which I have always received from my friends cannot be expressed in words and I feel lucky to be blessed with such wonderful friends.

I would also like to acknowledge the funding agency MHRD of Government of India for financial assistant in various forms.

It fills me with a deep sense of reverence when I think about my parents and my preceptor. Their constant encouragement, moral support and co-operation at every step of my life cannot be expressed in words. I am thankful for their love and blessings. My special thanks are also to my lovely wife, son (Narayan), sister, brother in law and niece (Archi) for their love and affection.

And lastly, I wish to thank all my friends and relatives along with the persons whose names have not been included on this piece of paper for extending their cooperation directly or indirectly.

  
(Saurabh Singh)

This thesis represents a culmination of work and better understanding in the field of solid oxide fuel cell (SOFC) that has taken place in the last couple of years. Energy markets are dominated by a substantial increase in energy demand due to the strong economic growth in the developing countries in all over the world. Ecological degradation and limited fossil fuel have compelled the governments and industries around the world into considering renewable energy technologies as alternatives to fossil fuels for power and electricity production. Elimination of pollutants, pollution of air by releasing toxic gases and compounds, and the groundwater by leaking fuel tanks with toxic-fuel additives (used to reduce pollutants) are also the subject of concern. Alternate energy resources are considered a long-term solution to the world's future energy demands, as they are environment-friendly and independent of our declining limited natural resources. All the issues that are associated with the burning of fossil fuels and hydrocarbon fuel sources can be under control by the fuel cells. Among the available renewal energy resources, a fuel cell is an emerging field for power production.

A fuel cell is an electrochemical device that converts chemical energy into electrical energy by utilizing the natural tendency of oxygen and hydrogen to react. Fuel cells are classified on the basis of electrolytes and operating temperatures. Among the various fuel cell technologies, SOFC utilizes the solid ceramic oxide components and is an important energy conversion device that generates electrical power by continuously converting chemical energy of fuel into electrical energy along with high energy conversion efficiency. There are mainly three components of SOFC: Anode, Cathode and Electrolyte.

In the present research work, the development of ceramic perovskite materials as anode for intermediate temperature solid oxide fuel cell (IT-SOFC) has been selected for

further investigation. Anode material is an essential component of SOFCs which exhibits high electrical conductivity in both atmospheres namely oxidizing and reducing. There are four primary requirements as given below, that any anode material in a SOFC must exhibit.

- The material must be porous enough to allow fuel to flow towards the electrolyte.
- The material must possess electronic conductivity to transport electrons throughout the electrode and the external circuit.
- It must have ionic conductivity too so that the  $O^{2-}$  anions are able to migrate throughout the electrode.
- Catalytic activity is necessary in order to facilitate the dissociation of oxygen and the oxidation of fuel.

However, in anode material, ions coming from the electrolyte flow through the anode and combine with fuel ( $H_2$ ) and release electrons at the region where the last three properties meet. It is often referred to as the triple phase boundary (TPB). Therefore, the large triple phase boundary is also required for anode materials for SOFC application. Further, an anode should have compatible thermal expansion coefficient (TEC) to that of other components of SOFC with the chemical stability.

On the basis of the above requirements, perovskite oxide with structure  $ABO_3$  is of great interest of research for their wide applicability in various device applications such as anode materials for solid oxide fuel cells. Therefore, in the investigation of low cost and widely stable materials, perovskite structured  $SrTiO_3$  has also been proposed as a potential anode for SOFCs under doping with rare earth elements. Its electronic conductivity is sufficient for the use as an anode at operating temperature of SOFC. This material offers not only high electronic conductivity but also optimum ionic conductivity.

Thus, SrTiO<sub>3</sub> with suitable doping has been proposed as promising nickel-free anode material for solid oxide fuel cell to resolve the issue of carbon and sulphur tolerance.

In order to synthesize SrTiO<sub>3</sub> based anode materials, solid state reaction and chemical reaction routes have been opted. Citrate-nitrate auto-combustion method of chemical reaction route is very important synthesis techniques over others to get particle in nano range and to reduce operating temperature. Structural, microstructural and elemental analyses have been carried out using XRD, FESEM and XPS techniques. Differential impedance analysis technique has been implemented to study the electrical behaviour and to understand the conduction mechanism.

In order to enhance the conductivity of SrTiO<sub>3</sub>, it was planned to synthesize doped SrTiO<sub>3</sub> at Sr-site with various rare earth elements (i.e. La, Y, Sm, and Dy). It is reported that the acceptor doping in the perovskite materials enhances the ionic conductivity whereas, the donor doping increases the electronic conductivity. Various rare earth element ions (i.e. La<sup>3+</sup>, Y<sup>3+</sup>, Sm<sup>3+</sup> and Dy<sup>3+</sup>) may act as donor dopant at Sr<sup>2+</sup> site of the SrTiO<sub>3</sub>, and suitable for substitution due to less difference between ionic radii. As the results of doping, two phenomena occur simultaneously, first maintain electro-neutrality in lattice defect structure due to charge imbalance and second improve the electrical conductivity of SrTiO<sub>3</sub> via the formation of oxygen-rich planes. In addition to that, redox coupling between Ti<sup>4+</sup> and Ti<sup>3+</sup> that also occurs in the system contributes to improving the electrical conductivity under reducing atmosphere and shows an n-type semiconducting behaviour.

The main emphasis of the present work is to develop cost effective novel anode materials for IT-SOFC with high conductivity at intermediate temperature range. For this purpose, strontium titanate material has been selected as a base material. The prime objective of the present thesis is to understand the electrical conduction mechanism in

rare earth doped SrTiO<sub>3</sub> systems and correlate it with the structural characteristics of the systems to make it more suitable as anode materials for IT-SOFC.

The present thesis is divided into seven chapters as per the brief description given below:

**Chapter-1** of this thesis illustrates motivation of the work, backgrounds of solid oxide fuel cell (SOFC), essential requirements of the anode for SOFC, present scenario of ceramic-perovskite anodes, strontium titanate based anode materials on the basis of the literature survey. This chapter includes also the main objectives of the present work.

**Chapter-2** represents the details of the employed experimental instruments and analysis techniques. Solid state reaction and chemical reaction technique were used to synthesize the rare earth doped SrTiO<sub>3</sub> systems. A detailed description of the employed instruments like XRD, FESEM, XPS and Impedance Spectroscopy etc. along with important analysis techniques like Rietveld refinement, differential impedance analysis have been discussed in this section.

**Chapter-3** describes the large polaron hopping phenomenon in La-doped SrTiO<sub>3</sub> anode material with a few compositions of La<sub>x</sub>Sr<sub>1-x</sub>TiO<sub>3-δ</sub> (with x = 0.0, 0.1, 0.2, 0.3, and 0.4) system which were synthesized via solid state reaction route. In order to study the conduction mechanism, the conductivity spectra of the system at different temperatures have been analyzed using Jonscher's power law and Ghosh scaling model along with the experimental verification of small and large polaron conduction using polaron tunneling model.

**Chapter-4** describes the structural and electrical conduction behaviour of Y-doped SrTiO<sub>3</sub> anode material for SOFC application in which Y<sub>x</sub>Sr<sub>1-x</sub>TiO<sub>3-δ</sub> (with x = 0, 0.03, 0.05, 0.08 and 0.1) compositions were synthesized via citrate-nitrate auto-combustion route. In order to propose the promising anode, the electrical conductivity and phase stability in air and hydrogen atmospheres were investigated through electrochemical

impedance spectroscopy and XRD measurements with corresponding FESEM micrographs, respectively.

**Chapter-5** describes the conduction mechanism in Sm-doped SrTiO<sub>3</sub> anode for SOFCs along with correlation between structural and electrical properties. The various compositions of Sm<sub>x</sub>Sr<sub>1-x</sub>TiO<sub>3-δ</sub> (with x = 0.05, 0.15 and 0.2) system were synthesized by citrate-nitrate auto-combustion route. The effect of Sm<sup>3+</sup> doping on electrical conductivities was studied for promising anode. The conductivity spectra of the system at different temperatures have been analyzed using Jonscher's power law and conduction mechanism has been explained qualitatively in terms of scaling behaviour.

**Chapter-6** describes the structural and electrical properties of Dy-doped SrTiO<sub>3</sub> as a promising anode material for SOFCs. In this chapter, Dy<sub>x</sub>Sr<sub>1-x</sub>TiO<sub>3-δ</sub> (with x = 0.03, 0.05, 0.08 and 0.1) compositions were synthesized by citrate-nitrate auto-combustion route. To understand the effect of Dy-content, anodic properties are measured in both air and hydrogen atmosphere, and explained in terms of defect chemistry.

**Chapter-7** describes the summary of the present thesis and future perspectives of the present research work. It has been concluded that SrTiO<sub>3</sub> based materials are cost effective and highly conductive and found that their suitability as an anode material for Intermediate Temperature Solid Oxide Fuel Cells (IT-SOFCs).

---

# CONTENTS

---

<b>Certificate</b>	<b>i</b>
<b>Declaration by the Candidate</b>	<b>ii</b>
<b>Copyright Transfer Certificate</b>	<b>iii</b>
<b>Acknowledgements</b>	<b>iv</b>
<b>Preface</b>	<b>vi</b>
<b>Contents</b>	<b>xi</b>
<b>List of Figures</b>	<b>xiv</b>
<b>List of Tables</b>	<b>xix</b>
<b>Abbreviations</b>	<b>xxi</b>
<b>Chapter 1: Introduction and Literature Review</b>	<b>1-28</b>
1.1 Overview of the Field	1
1.2 Fuel Cell	2
1.3 Types of Fuel Cell	4
1.4 Solid Oxide Fuel Cell (SOFC)	6
1.5 Operation of SOFC	6
1.6 Types of Solid Oxide Fuel Cells (SOFCs)	8
1.6.1 High Temperature Solid Oxide Fuel Cell (HT-SOFC)	8
1.6.1.1 Disadvantages of HT-SOFC	9
1.6.2 Intermediate Temperature Solid Oxide Fuel Cell (IT-SOFC)	9
1.6.2.1 Advantages of IT-SOFC	9
1.7 Material Selection for SOFCs	10
1.7.1 Electrolyte Material	10
1.7.2 Cathode Material	11
1.7.3 Interconnect Material	11
1.7.4 Anode Material	12
1.8 Perovskite Oxide Systems for Anode Materials	13
1.9 Types of Perovskite Oxides	13
1.9.1 $A^{1+}B^{5+}O_3$ Type Structure	14
1.9.2 $A^{2+}B^{4+}O_3$ Type Structure	14
1.9.3 $A^{3+}B^{3+}O_3$ Type Structure	14
1.9.4 $A^{4+}B^{2+}O_3$ Type Structure and $A^{5+}B^{1+}O_3$ Type Structure	15
1.10 The Essential Requirements of Anode Material in SOFC	17
1.11 Ceramic Perovskite over Ni-Cermet Anode Materials	18
1.12 Donor-doped SrTiO <sub>3</sub> Systems as Anode Materials	20
1.13 Conduction Mechanism in the SrTiO <sub>3</sub> Perovskite Systems	22
1.13.1 Ionic Conduction	22
1.13.2 Electronic Conduction	25
1.14 The Main Objectives of Research Work	27

<b>Chapter 2: Synthesis, Characterization and Analysis Techniques</b>	<b>29-54</b>
2.1 Overview	29
2.2 Synthesis and Characterization Techniques	30
2.3 Synthesis of Materials	31
2.3.1 Preparation of Nitrates	31
2.4 Synthesis Routes	31
2.4.1 Solid State Reaction Route	32
2.4.2 Chemical Reaction Routes	33
2.4.2.1 Auto-Combustion Route	34
2.4.2.2 Sol-Gel Technique	34
2.4.2.3 Citrate-Nitrate Auto-Combustion synthesis	34
2.5 Characterizations Techniques	35
2.5.1 Phase Formation and Crystal Structure Studies by Powder X-Ray Diffraction	36
2.5.2 Density and Porosity Measurements	39
2.5.3 Microstructural Studies by Field Emission Scanning Electron Microscopy (FESEM) and Electron Dispersion Spectroscopy (EDS)	40
2.5.4 X-ray Photoelectron Spectroscopy	41
2.6 Conductivity Measurement	43
2.6.1 Conductivity Measurements in Air using Impedance Analyser	43
2.6.2 Electrical Measurements in Reducing Atmosphere using ProboStat	44
2.7 Analysis Techniques	46
2.7.1 Phase Formation Study by Rietveld Refinement Technique	46
2.7.2 Process of Analysing FESEM and XPS Study	47
2.7.3 Electrical Properties	48
2.7.3.1 Conductivity Spectroscopic Technique	48
2.7.3.2 Impedance Spectroscopic Technique	50
<b>Chapter 3: Study of Conduction Mechanism in La-doped SrTiO<sub>3</sub> Anode Materials</b>	<b>55-71</b>
3.1 Introduction	55
3.2 Results and Discussion	56
3.2.1 Structural Studies	56
3.2.2 Density and Micro Structural Studies	59
3.2.3 Electrical Conductivity	60
3.2.4 Conduction Mechanism	63
3.2.5 Modulus Analysis	66
3.2.6 Photoluminescence Analysis	68
3.2.7 Evidence of Polaron Size from Structural Data	69
3.3 Conclusions	71
<b>Chapter 4: Structural and Electrical Properties of Y-doped SrTiO<sub>3</sub> Anode Materials</b>	<b>73-86</b>
4.1 Introduction	73
4.2 Results and Discussion	74

4.2.1 Structural Studies	74
4.2.2 Microstructural Analysis	77
4.2.3 XPS Analysis	78
4.2.4 Impedance Analysis	80
4.2.5 Chemical Stability	84
4.3 Conclusions	85
<b>Chapter 5: Structural and Electrical Properties of Sm-doped SrTiO<sub>3</sub>     Anode Materials</b>	<b>87-99</b>
5.1 Introduction	87
5.2 Results and Discussion	88
5.2.1 Structural Studies	88
5.2.2 Microstructural Analysis	91
5.2.3 XPS Analysis	92
5.2.4 Impedance Analysis	94
5.2.5 Chemical Stability	98
5.3 Conclusions	99
<b>Chapter 6: Structural and Electrical Properties of Dy-doped SrTiO<sub>3</sub>     Anode Materials</b>	<b>101-112</b>
6.1 Introduction	101
6.2 Results and Discussion	102
6.2.1 Structural Studies	102
6.2.2 Microstructural Analysis	104
6.2.3 Impedance Analysis and Chemical Stability	105
6.3 Conclusions	112
<b>Chapter 7: Conclusion and Future Perspectives</b>	<b>113-116</b>
7.1 Conclusion of the Present Investigation	113
7.2 New Directions and Future Perspectives	115
<b>References</b>	<b>117-136</b>
<b>List of Publications/Conferences</b>	<b>137-138</b>

---

## LIST OF FIGURES

---

		Page No.
<b>Chapter 1</b>	<b>Introduction and Literature Review</b>	
Figure 1.1	World energy demand (in BTUs) and its electricity consumption for different sectors.	1
Figure 1.2	Comparison of power output efficiency.	3
Figure 1.3	Summary of different types of fuel cell.	5
Figure 1.4	Working principle of SOFC.	7
Figure 1.5	(a) Perovskite structure $ABO_3$ and (b) octahedron $BO_6$ .	13
Figure 1.6	Triple phase boundary (TPB) and anodic reaction.	18
Figure 1.7	A schematic representation of the conductivity behaviour of an oxide ion conductor.	24
<b>Chapter 2</b>	<b>Synthesis, Characterizations and Analysis Techniques</b>	
Figure 2.1	Block diagram of various synthesis techniques.	31
Figure 2.2	The image diagram representing the steps of solid state reaction method.	32
Figure 2.3	Diagram representation of chemical reaction route with the appropriate steps.	33
Figure 2.4	Block diagram of various Characterizations and analysis techniques.	36
Figure 2.5	Schematic diagram of Bragg's law occurring through a crystal lattice.	37
Figure 2.6	The construction of X-ray diffractometer with image of Rigaku (Miniflex 600) X-ray diffractometer.	38
Figure 2.7	The density measurement kit (Denver SI-234).	39
Figure 2.8	Schematic diagram of FESEM with image of FEI (NOVA NANOSEM 450).	41
Figure 2.9	A Schematic diagram of XPS (X-ray photoelectron spectroscopy).	42
Figure 2.10	A Schematic design of XPS (X-ray photoelectron spectroscopy) working with photograph of XPS setup	

(KRATOS Amicus model).

43

Figure 2.11 Computer controlled automated impedance analyser setup along with sample holder and furnace (6500 P Wayne Kerr, UK).

44

Figure 2.12 The Probostat (Norecs, Norway) system impedance Analyzer (FRA, mod. SOLARTRON 1250 - Schlumberger), in a range of frequency between 1-10<sup>6</sup> Hz.

45

Figure 2.13 A typical conductivity spectra of a polycrystalline material.

50

Figure 2.14 Equivalent circuit for a polycrystalline ceramic sample and corresponding frequency response in the Nyquist plots.

54

### **Chapter 3 Study of Conduction Mechanism in La-doped SrTiO<sub>3</sub> Anode Materials**

Figure 3.1 Rietveld refinement of X-ray diffraction pattern of La<sub>x</sub>Sr<sub>1-x</sub>TiO<sub>3</sub> (0.0 ≤ x ≤ 0.40) system sintered at 1400 °C.

57

Figure 3.2 SEM image of fractured surface of the sintered pellet of the compositions (a) LST0 (b) LST1 (c) LST2 (d) LST3 and (e) LST4.

59

Figure 3.3 Frequency dispersion of Conductivity spectra for LST0, LST1, LST2 and LST3 compositions in the temperature range from 400 °C to 600 °C.

60

Figure 3.4 Arrhenius Plot of La<sub>x</sub>Sr<sub>1-x</sub>TiO<sub>3</sub> (0.0 ≤ x ≤ 0.30).

62

Figure 3.5 Variation of critical exponent n in La<sub>x</sub>Sr<sub>1-x</sub>TiO<sub>3</sub> (0.0 ≤ x ≤ 0.30) compositions as a function of temperature.

64

Figure 3.6 Scaled conductivity spectra of the compositions (a) LST0 (b) LST1 (c) LST2 and (d) LST3 in the temperature range from 400 °C to 600 °C..

65

Figure 3.7 The dc conductivity ( $\sigma_{dc}$ ) vs. hopping frequency ( $\nu_H$ ) for LST0, LST1, LST2 and LST3 compositions.

66

Figure 3.8 Variation of M'' and Z'' with frequency (log  $\nu$ ) for (a) LST0, (b) LST1 and (c) LST2 compositions at 480 °C.

67

Figure 3.9 Photoluminescence spectra of La<sub>x</sub>Sr<sub>1-x</sub>TiO<sub>3</sub> (0.0 ≤ x ≤ 0.30) samples.

69

Figure 3.10	(a) Variation of intensity of XRD peak with $2\theta-\delta$ ( $^\circ$ ) where $d$ is the angle at which maxima occurs showing diffuseness of XRD peak (110) with composition, (b) Variation of microstrain and crystallite size with $x$ (c) Variation of coherence length and lattice constant with $x$ .	70
<b>Chapter 4</b>	<b>Structural and Electrical Properties of Y-doped SrTiO<sub>3</sub> Anode Materials</b>	
Figure 4.1	(a) XRD patterns of the sintered samples of the system Y <sub>x</sub> Sr <sub>1-x</sub> TiO <sub>3</sub> (i.e, YST0, YST3, YST5, YST8, and YST10) (b) Angle shift of (110) peak with the Y doping.	75
Figure 4.2	Secondary phase concentration, X <sub>s</sub> , as function of $x \geq 0.03$ in Y <sub>x</sub> Sr <sub>1-x</sub> TiO <sub>3-<math>\delta</math></sub> (b) Variation of lattice parameter with tolerance factor, (c) The variation of intensity of XRD peak (110) via $2\theta-\delta$ ( $^\circ$ ) with compositions ( $x$ ) for Y <sub>x</sub> Sr <sub>1-x</sub> TiO <sub>3-<math>\delta</math></sub> system, and (d) The variation of microstrain and crystallite size with compositions ( $x$ ).	77
Figure 4.3	FESEM images of fractured samples sintered at 1200 $^\circ$ C in air for (a) YST0 (b) YST3 (c) YST5 (d) YST8 and (e) YST10.	78
Figure 4.4	(a) The XPS survey spectra of Y-doped SrTiO <sub>3</sub> (b) The O-1s core level spectra (c) The XPS spectra of Ti 2p of YST5 sample.	80
Figure 4.5	The Arrhenius plot of $\log \sigma T$ vs. $1000/T$ (a) in O <sub>2</sub> atmosphere (b) in H <sub>2</sub> atmosphere.	81
Figure 4.6	XRD patterns of Y-doped SrTiO <sub>3</sub> samples before and after reducing atmosphere and inset FESEM micrographs of reduced samples.	85
<b>Chapter 5</b>	<b>Structural and Electrical Properties of Sm-doped SrTiO<sub>3</sub> Anode Materials</b>	
Figure 5.1	The tolerance factor with the compositions.	88
Figure 5.2	(a) The XRD patterns of the sintered samples in air and (b) The shifting of diffraction peaks towards higher angle.	89

Figure 5.3	(a) Variation of intensity of XRD peak with $2\theta-\delta$ ( $^\circ$ ) where $\delta$ is the angle at which maxima occurs showing diffuseness of XRD peak (110) with the compositions, (b) Variation of lattice parameter and relative density with the compositions and (c) Variation of microstrain and crystallite size with the compositions.	90
Figure 5.4	The EDAX mapping of the FESEM micrographs as shown in inset of the fractured samples (a) SST5, (b) SST15, (c) SST20 and (d) The stoichiometric and EDAX atomic % for the samples.	92
Figure 5.5	(a) The XPS wide spectra of Sm-doped $\text{SrTiO}_3$ samples and (b) The illustration of O 1s core level spectra of the samples.	93
Figure 5.6	(a) The electrical conductivity spectra with JPL fitting and (b) The Ghosh scaling of conductivity spectra with inset of Summerfield scaling at measured temperatures of the sample SST5.	95
Figure 5.7	The complex impedance Nyquist plots of the sample SST5 at measured temperatures.	96
Figure 5.8	(a) The Arrhenius plot ( $\log \sigma T$ vs. $1000/T$ ) for the all studied samples and (b) The comparative Arrhenius plot with inset conductivity plot at $600^\circ\text{C}$ for the sample SST15 in $\text{O}_2$ and $\text{H}_2$ atmospheres.	97
Figure 5.9	XRD patterns of unreduced and reduced samples and inset FESEM micrographs of reduced samples.	98
<b>Chapter 6</b>	<b>Structural and Electrical Properties of Sm-doped <math>\text{SrTiO}_3</math> Anode Materials</b>	
Figure 6.1	Rietveld refinement (-) of XRD patterns ( $\square = \text{DST3}$ , $\circ = \text{DST5}$ , $\Delta = \text{DST8}$ and $+$ = DST10). Residuals (Res) and Miller indexes are also reported with major reflections of $\text{TiO}_2$ ( $\wedge$ ), $\text{Dy}_2\text{O}_3$ ( $\#$ ) and $\text{Dy}_2\text{Ti}_2\text{O}_7$ ( $*$ ) secondary phases.	103
Figure 6.2	The calculated microstrain and crystallite size as function of Dy amount.	104

Figure 6.3	The FESEM micrographs of fractured compositions (a) DST3, (b) DST5, (c) DST8 and (d) DST10.	105
Figure 6.4	Impedance spectra of DST3 sample, measured in air, at: ( $\Delta$ ) 232 °C, ( $\square$ ) 305 °C, ( $\circ$ ) 380 °C.	107
Figure 6.5	Nyquist plot of impedances measured in air, at several temperatures, as reported by symbols: ( $\Delta$ ) DST10 at 459 °C, ( $\square$ ) DST5 at 174 °C, ( $\circ$ ) DST3 at 232 °C, ( $\text{ )}$ DST8 at 515 °C. The solid line was obtained by fitting the data with the equivalent circuit, as reported in the text. Dark markers point at measurement frequency.	107
Figure 6.6	Arrhenius plot of conductivity of DST3 ( $\bullet$ ), DST5 ( $\blacktriangle$ ), DST8 ( $\blacksquare$ ) and DST10 ( $\blacktriangledown$ ), samples as function of temperature, in air (full symbols) and in hydrogen (empty symbols). Lines are the best fit of Arrhenius relation to experimental data.	108
Figure 6.7	Comparison of XRD patterns obtained before (thin line) and after reduction (thick line). Miller indexes of SrTiO <sub>3</sub> are also reported with major reflections of TiO <sub>2</sub> ( $\wedge$ ), Dy <sub>2</sub> O <sub>3</sub> ( $\#$ ) and Dy <sub>2</sub> Ti <sub>2</sub> O <sub>7</sub> ( $\ast$ ) secondary phases. Peaks of mixed Ti, Sr oxides, different from SrTiO <sub>3</sub> are highlighted by rectangles.	111
<b>Chapter 7</b>	<b>Conclusions and Future Scope</b>	
Figure 7.1	The comparative electrical conductivity of promising anodes at 650 °C in hydrogen atmosphere.	115

---

## LIST OF TABLES

---

		Page No.
<b>Chapter 1</b>	<b>Introduction and Literature Review</b>	
Table 1.1	Reactions occurring at anode and cathode for all five types of fuel cells	5
Table 1.2	Electrical conductivity of some chromite and titanate based perovskite ceramic materials in reducing atmosphere.	20
<b>Chapter 2</b>	<b>Synthesis, Characterizations and Analysis Techniques</b>	
Table 2.1	Specifications of the raw materials with their grades, purity and manufacturer used for preparation of various electro-ceramic samples.	30
Table 2.2	Starting materials and firing schedule for various compositions.	30
<b>Chapter 3</b>	<b>Study of Conduction Mechanism in La-doped SrTiO<sub>3</sub> Anode Materials</b>	
Table 3.1	Structural parameters, relative density and the goodness of fitting parameters of the LST system.	58
Table 3.2	Electrical conductivity and Activation energy of the LST system.	61
<b>Chapter 4</b>	<b>Structural and Electrical Properties of Y-doped SrTiO<sub>3</sub> Anode Materials</b>	
Table 4.1	Activation energy, relative density and adsorbed oxygen of YST samples.	82
<b>Chapter 5</b>	<b>Structural and Electrical Properties of Sm-doped SrTiO<sub>3</sub> Anode Materials</b>	
Table 5.1	The lattice parameter, cell volume, Rietveld refined	

	parameters and % porosity of the studied samples.	90
Table 5.2	Activation energy and lattice oxygen content of all the studied samples.	97
<b>Chapter 6</b>	<b>Structural and Electrical Properties of Dy-doped SrTiO<sub>3</sub> Anode Materials</b>	
Table 6.1	Rietveld refined parameters and relative density of studied compositions.	105
Table 6.2	Conductivity values ( $\sigma$ ) measured at 650 °C and calculated energy activations ( $E_a$ ) of conduction mechanism, for all composition, respectively in air and in hydrogen.	107

---

## LIST OF ABBREVIATIONS

---

SOFC	:	Solid Oxide Fuel Cell
PEMFC	:	Polymer Electrolyte Membrane Fuel Cell
AFC	:	Alkaline Fuel Cell
PAFC	:	Phosphoric Acid Fuel Cell
MCFC	:	Molten Carbonate Fuel Cell
HT-SOFC	:	High Temperature Solid Oxide Fuel Cell
IT-SOFC	:	Intermediate Temperature Solid Oxide Fuel Cell
SSR	:	Solid State Reaction Route
CR	:	Chemical Reaction Route
LST	:	Lanthanum Doped Strontium Titanate
YST	:	Yttrium Doped Strontium Titanate
SST	:	Samarium Doped Strontium Titanate
DST	:	Dysprosium Doped Strontium Titanate
YSZ	:	Yttrium Stabilized Zirconia
PVA	:	Poly Vinyl Alcohol
JPL	:	Jonscher's Power Law
TEC	:	Thermal Expansion Coefficient
TPB	:	Triple Phase Boundary
XRD	:	X-Ray Diffraction
FESEM	:	Field Emission Scanning Electron Microscope
EDS	:	Electron Dispersion Spectroscopy
HRTEM	:	High Resolution Transmission Electron Microscope
XPS	:	X-ray Photoelectron Spectroscopy